The Li^+ Cation—The Descendant of H^+ or an Ancestor of Na^+? The Properties of Li^+Ar_n ($n = 1-6$) Clusters

Jaroslaw J. Szymczak,[†,‡] Kalathingal T. Giju,[†] Szczepan Roszak,[†,‡] and Jerzy Leszczynski*[,†]

Computational Center for Molecular Structure and Interactions, Department of Chemistry, Jackson State University, P.O. Box 17910, Jackson, Mississippi 39217, and Institute of Physical and Theoretical Chemistry, Wroclaw University of Technology, Wyb. Wyspianskiego 27 50-370 Wroclaw, Poland

Received: February 27, 2004; In Final Form: June 1, 2004

Ab initio studies of molecular structures and properties of the Li^+Ar_n complexes were carried out. The investigation of the Li^+Ar dimer with the MP2(FULL)/6-311G+(3df) method provides satisfactory agreement with the available experimental data. This conclusion is extrapolated for larger Li^+Ar_n ($n > 1$) clusters which are studied within this level of theory. The reported complexes are stable and deserve the future experimental efforts. The obtained results indicate that the consecutive complexes represent the most symmetrical structures possible with the closing shell for the Li^+Ar_6 cation. The dissociation energies as well as interaction energy components follow systematic paths of changes. The reveled clusters are different from their H^+Ar_n predecessors characterized by two solvation shells of 7 ligands total and are also different from Na^+Ar_n clusters for which the single shell may accommodate eight argons. The Ar−Ar interactions do not influence geometries of small complexes but are noticeable in larger structures due to repulsive forces caused by the lack of space around the central cation.

I. Introduction

The Li^+Ar complex has been extensively studied experimentally including beam scattering,[1,2] ion mobility,[3,4] and vacuum ultraviolet (VUV) emission spectroscopy.[5] Experimental mobility and diffusion coefficient data lead to the potential energy curves. The theoretically determined potential curves, needed to verify experimental findings, were also extensively studied.[6−10] The measured values of dissociation energies vary from 6.4 to 7.3 kcal/mol. Such a range of experimental values indicates difficulties in providing accurate data for the noble gas complexes. The further cluster growth by the attachment of argon atoms to the charged metallic center is also possible. Although not for the Li^+, other clusters of Group I − inert gas complexes were observed. The Ar_2H^+ complex was detected spectroscopically in the argon matrix.[11] The potassium based clusters of different rare gases were detected by the time-of-flight (TOF) spectrometry.[12] The theoretical studies for H^+Ar_n and Na^+Ar_n are also available.[13−16] The complexation of Ar atoms to Li^+ yeilding alkali ion−inert gas complexes may play an important role in the chemistry of the earth's mesosphere and in the chemistry of plasma. Theoretically, availability of reliable Li^+Ar_n cluster parameters is useful in the development of potential parameters for molecular dynamics simulations. The comparison of structures and other properties reveals the striking differences between H^+ and Na^+ originating complexes. The studies of Li^+Ar_n clusters may answer the question of the source of such differences.

In the present work, we investigate the Li^+Ar_n ($n = 1-6$) structures at the MP2 level using the extended basis set. The thermodynamics of complexes and vibrational properties are studied. The nature of bonding is discussed based on the electronic population analysis and interaction energy components. The results were compared with the data available for H^+Ar_n and Na^+Ar_n complexes in order to elucidate similarities and differences within the Group I moieties.

II. Theoretical Methods

The geometries of complexes have been optimized at the MP2(FULL) level.[17] For the dissociation energies, the single point calculations were performed at the CCSD(T,FULL) approach[18,19] using the equilibrium geometry obtained from the MP2(FULL) optimization. The largest known in the literature basis sets applied for the Li^+Ar complex[10] are not feasible for extended clusters. A series of 6-31+G(d), 6-311+G(d), 6-311+G(df), 6-311+G(2df), and 6-311+G(3df) basis sets[20] were analyzed for the Li^+Ar dimer. The 6-311+G(3df) basis was found to be reasonably saturated, although the dissociation energy difference between 6-311G+(2df) and 6-311+G(3df) still amounts to 0.32 kcal/mol (calculated at the CCSD(T) level). The corresponding bond change is 0.018 Å. All electrons are correlated in both methods applied as a core-valence error leads to the discrepancy of 0.44 kcal/mol and 0.026 Å in D_e and r_e, respectively. The advanced correlation treatment (CCSD(T)) has little impact on MP2 calculated values, mainly $\Delta D_e = 0.03$ kcal/mol and $\Delta r_e = 0.004$ Å. In further studies of the complexation the 6-311+G(3df) basis set is utilized in the conjunction with the post Hartree−Fock methods, thus taking care of the radial and angular correlation parts of the Li and Ar atoms. Although, the BSSE correction has significant impact on interaction energies, its structural influence on studied complexes was found insignificant. The theoretically determined equilibrium distance (3.775 Å) and the bond dissociation energy (99.19 cm^{-1}) in the Ar_2 dimer are in an excellent agreement with experimental data[21] of 3.761 Å and 99.2 cm^{-1}, respectively. The harmonic vibrational frequencies, calculated at MP2 level,

* Corresponding author phone: (601)979-7824; fax: (601)979-7823; e-mail: jerzy@ccmsi.us.
† Jackson State University.
‡ Wroclaw University of Technology.

10.1021/jp049103k CCC: $27.50
Published on Web 07/14/2004

TABLE 1: Successive Dissociation Energies (kcal/mol) without (D_e) and with ZPE (D_0) Corrections along with BSSE Corrections ($D_{e(BSSE)}$ and $D_{0(BSSE)}$), Successive Dissociation Enthalpy (ΔH at 298.15 K, kcal/mol), and Successive Dissociation Entropy (ΔS at 298.15 K, cal/mol-K) at the MP2(FULL)//MP2(FULL)/6-311+G(3df) and CCSD(T,FULL)//MP2(FULL)/6-311+G(3df) Levels

	MP2			
complex	D_e/D_0 ($D_{e(BSSE)}/D_{0(BSSE)}$)	ΔH	ΔS	CCSD(T) D_e
$ArLi^+$ ($C_{\infty v}$)	6.88/6.50 (6.07/5.60)	7.10	20.92	7.01
Ar_2Li^+ ($D_{\infty h}$)	6.74/6.45 (5.58/5.29)	6.38	11.57	6.88
Ar_3Li^+ (D_{3h})	6.46/5.99 (5.15/4.68)	6.38	24.42	6.54
Ar_4Li^+ (T_d)	6.12/5.71 (4.62/4.21)	5.78	23.95	6.11
Ar_5Li^+ (C_{4v})	3.68/3.54 (2.09/1.95)	3.44	20.09	3.40
Ar_6Li^+ (O_h)	4.87/4.62 (3.05/2.80)	4.58	29.14	

TABLE 2: Vibrational Frequencies (cm^{-1}) and IR Intensities (KM/mol) of the Complexes Calculated at the MP2(FULL)/6-311+G(3df) Level

complex	frequencies
$ArLi^+$ ($C_{\infty v}$)	267 (σ_g, 151)
Ar_2Li^+ ($D_{\infty h}$)	8 (π_u, 74), 102 (σ_g, 0), 351 (σ_u, 202)
Ar_3Li^+ (D_{3h})	22 (E′, 3), 38 (A2″, 56), 101 (A1′, 0), 308 (E′, 135)
Ar_4Li^+ (T_d)	24 (E, 0), 36 (T_2, 4), 101 (A_1, 0), 275 (T_2, 104)
Ar_5Li^+ (C_{4v})	7 (B2, 0), 37 (E, 0), 55 (A1, 3), 67 (B1, 0), 67 (B2, 0), 68 (E, 2), 97 (A1, 0), 226 (A1, 82), 228 (E, 127)
Ar_6Li^+ (O_h)	38 (T_{2u}, 0), 56 (T_{2g}, 0), 69 (E_g, 0), 70 (T_{1u}, 2), 96 (A_{1g}, 0), 212 (T_{1u}, 116)

have been used for the characterization of stationary points and zero-point energy (ZPE) corrections. All the stationary points have been identified as local minima. The choice of 6-311+G(3df) is consistent with the former calculations[14−16] for H^+Ar_n and Na^+Ar_n and should allow for systematic comparison of properties within Group 1 metals. The level of calculations, when applied for larger complexes, constitutes the present "State of the Art" approach.[22]

The intermolecular interactions were studied using the hybrid variational-perturbational interaction energy decomposition scheme.[23−25] In this approach the SCF interaction energy is partitioned into the first-order electrostatic $\epsilon_{el}^{(10)}$, Heitler-London exchange ϵ_{ex}^{HL}, and the higher order delocalization ΔE_{del}^{HF} energy term.

$$\Delta E^{HF} = \epsilon_{el}^{(10)} + \epsilon_{ex}^{HL} + \Delta E_{del}^{HF} \qquad (1)$$

The ΔE_{del}^{HF} component accounts for the induction and exchange-induction effects associated with the relaxation of the electronic densities of monomers upon interaction, whereas the Heitler-London terms ($\epsilon_{el}^{(10)}$ and ϵ_{ex}^{HL}) represent the electrostatic interactions and exchange repulsion between the subsystems, which electron density distributions are unperturbed by the interaction with the partner. The electron correlation effects are taken into account by means of the Møller−Plesset perturbation theory. The $\epsilon_{MP}^{(2)}$ interaction energy term, which includes the dispersion contribution and correlation corrections to the Hartree−Fock components, is calculated in the supermolecular approach as a difference between the appropriate second-order MPPT energy corrections.

$$\epsilon_{MP}^{(2)} = E_{AB}^{(2)} - E_A^{(2)} - E_B^{(2)} \qquad (2)$$

All interaction energy terms are calculated consistently in the dimer centered basis set, and therefore they are free from the basis set superposition error (BSSE) due to the full counterpoise correction.[26,27] Such a scheme can be extended to molecular systems more complex than dimers. The total interaction energy of a system consisting of *n*-subunits can be expressed as a sum of the 2,3,...,*n* body interaction energies.[28−30] The total energy of interacting species can be defined as

$$E_{ABC} = \sum_{X=A,B,C} E_X + \sum_{X<Y} \Delta E_{XY} + \Delta E_3 \qquad (3)$$

where the first term on the right-hand side denotes the energy of free monomers, the second term represents the two-body term, and the third term denotes the three-body term. Taking into account additivity of electrostatic interactions and applicability of the Löwdin formula[31] for Heitler-London interaction energy to any *n*-body system,[32] such an approach can be applied also in the further decomposition of exchange, delocalization, and correlation components into 2,3...*n*-body contributions.[33]

Calculations for equilibrium geometries and vibrational frequencies have been performed using Gaussian 98 suite of codes.[34] The natural charges and natural valence electronic configuration were calculated using the NBO program included in the Gaussian package.[35] The interaction energy decomposition scheme was implemented[36] in the Gamess program.[37]

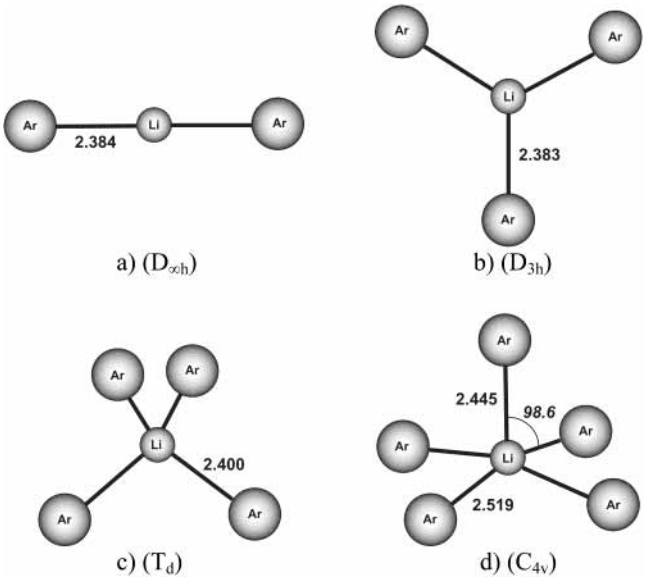

Figure 1. The molecular structures of (a) Li^+Ar_2; (b) Li^+Ar_3; (c) Li^+Ar_3; and (d) Li^+Ar_5 complexes. Bond distance in angstroms.

III. Structures and Energetics of Li^+Ar_n Complexes

1. Li^+Ar. The calculated bond distance (2.376 Å) agrees well with the available experimental values of 2.281 Å. The dissociation energy (D_e) of 6.31 kcal/mol (Table 1) is reasonably close to the value of 6.63 kcal/mol claimed by authors to be 0.3% within the error margin.[9] The dissociation energy is much smaller from that of H^+Ar (94.6 kcal/mol)[14] but is comparable to the value characterizing the Na^+Ar dimer (4.08 kcal/mol).[15] Consequently the stretching frequency mode of the Li−Ar interaction of 267 cm^{-1} (Table 2) is much lower compared to that of the H^+Ar bond of 2768 cm^{-1}.

2. Li^+Ar_2. The coordination of the second Ar to Li^+ leads to the linear $D_{\infty h}$ complex (Figure 1a) with the Li^+Ar bond characteristics almost identical to that found for the Li^+Ar dimer. The linear geometry indicates that the bond stabilization by covalent forces is higher than 0.3 kcal/mol—the possible energetical gain due to the Ar−Ar attraction.[21] The Na^+Ar_2 is

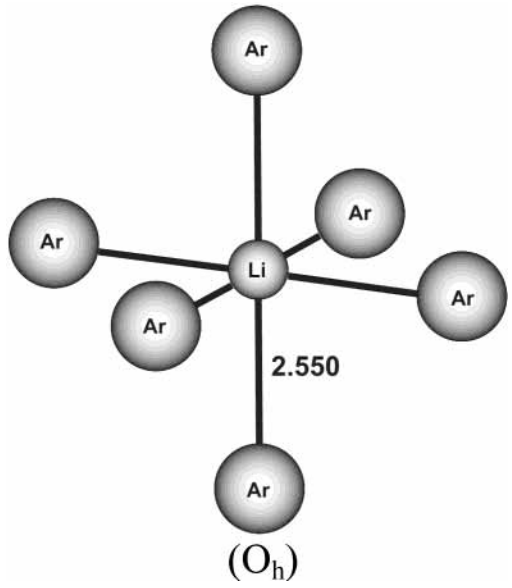

Figure 2. The geometry of Li^+Ar_6 cluster. Bond distance in angstroms.

very similar to Li^+Ar_2 with little change of bonding parameters due to the $NaAr^+ + Ar$ reaction. The proton bound dimer also possesses the $D_{\infty h}$ symmetry; however, its bonding characteristics differs significantly from H^+Ar with lower but still significant dissociation energy of 16.4 kcal/mol.

3. Li^+Ar_3. The Li^+Ar_3 complex possesses the symmetrical D_{3h} structure (Figure 1b) with the bond distance almost the same as one in the smaller clusters. The bond dissociation energy is only slightly lower from Li^+Ar_2. The Ar−Ar distance of 4.128 Å is longer from 3.761 Å observed in the Ar_2 dimer,[21] indicating that the structure is controlled by the Li^+−Ar bonding. The Li^+Ar_3 structure is different from H^+Ar_3 in which the Ar−H−Ar axis is preserved, and the third atom occupies the perpendicular plane.[14] This plane constituting new shell will not accept any further ligand reacting with the Ar−H−Ar^+ core. The Na^+Ar_3 is also different from Li^+Ar_3 with the C_{3v} structure significantly distorted to the C_{2v} skeleton. The symmetrical stretching vibration of Li^+Ar_3 is almost unchanged compared to the Li^+Ar_2 complex.

4. Li^+Ar_4. The Li^+Ar_4 cation again assumes the most symmetrical−tetrahedral structure (Figure 1c). The Li^+Ar bond is slightly longer compared to bonds in smaller clusters. The Ar−Ar distances are now comparable to the Ar−Ar bond in the dimer. The Li^+Ar_4 complex is again different from both H^+Ar_4 and Na^+Ar_4 continuing patterns of complexes containing three argons. The bond dissociation energy dissociation energy is slightly lower compared to that in Li^+Ar_3.

5. Li^+Ar_5. The C_{4v} pyramid constitutes the lowest isomer of Li^+Ar_5 (Figure 1d). The isomer of trigonal bipyramid is also stable; however, it is higher in energy. Due to the crowding of argon atoms the bond lengths increase by 0.1 Å (in longer) and 0.05 Å (in shorter) Li−Ar bonds. The bond increase balances the Ar−Ar distance shortening due to the lack of space around Li^+. The structural changes significantly influence the dissociation energy which decreases as much as 40%. The structure of the Li^+Ar_5 complex is similar to Na^+Ar_5. The H^+Ar_5 cation continues its pattern with filling the second shell, while Na^+Ar_5 also possesses the C_{4v} structure. The weakening of bonds is also visible as the slight decrease of the symmetric stretching vibrational mode.

6. Li^+Ar_6. The Li^+Ar_6 cluster again possesses the most symmetrical structure possible—O_h symmetry (Figure 2). The increase of Li^+Ar bonds balances the Ar−Ar exchange repulsion forces. The structure clearly represents the closing of the shell. None of the additional Ar may approach Li^+ within the bonding distance without prohibitatively short distances to other ligands. The closing of the shell is also visible as a slight increase of the dissociation energy and as an increase of the negative value of the incremental entropy. The geometry of Na^+Ar_6 is also represented by the tetragonal bipyramid although the size of Na^+ ions leading to longer Na−Ar bonds allows for larger clusters and the closing of the shell is not yet observed for $n = 6$. The H^+Ar_6 cluster allows for more ligands in its second shell. The symmetrical stretching vibration again decreases slightly. It indicates similarities of presented cluster to its predecessors.

TABLE 3: Mulliken Charges, Natural Charges, and Natural Valence Electron (NVE) Configuration Calculated Using the Density of MP2(FULL)/6-311+G(3df) Level

	Mulliken charge		natural charge		NVE				
					Li		Ar		
complex	Li	Ar	Li	Ar	2s	2p	3s	3p	3d
$ArLi^+$ ($C_{\infty v}$)	0.853	0.147	0.98	0.02	0.01	0.01	1.98	5.87	0.09
Ar_2Li^+ ($D_{\infty h}$)	0.742	0.129	0.96	0.02	0.03	0.01	1.98	5.86	0.09
Ar_3Li^+ (D_{3h})	0.676	0.108	0.91	0.03	0.07	0.02	1.98	5.86	0.09
Ar_4Li^+ (T_d)	0.620	0.095	0.86	0.04	0.11	0.03	1.98	5.86	0.09
Ar_5Li^+ (C_{4v})	0.635	0.075	0.85	0.03	0.12	0.03	1.98	5.86	0.09
		0.065[a]		0.03					
Ar_6Li^+ (O_h)	0.688	0.052	0.82	0.03	0.15	0.03	1.98	5.86	0.09

[a] The short bond, Figure 1d.

IV. Nature of Bonding

The electronic charges calculated from Mulliken population analysis illustrate the systematically decreasing electron transfer from the single Ar ligand to the central cation (Table 3). The decreasing charge on the central cation as a number of ligands grows is also indicated by natural bond analysis, although the similarity between both approaches is only qualitative. The important conclusion arises from the natural valence orbital occupation indicating the involvement in bonding is mostly s type electrons of lithium. The lack of directional orbitals involved in the bonding may be the reason to the formation of very symmetrical structures.

The interaction energy components provide a more precise picture regarding the nature of bonding in studied complexes. The interaction energies corresponding to the reaction $Li^+Ar_{n-1} + Ar = Li^+Ar_n$ of the growth of cluster are presented in Table 4. The increased interactions due to the crowding of ligands are visible for the largest ($n = 5,6$) complexes in electrostatic ($\epsilon_{el}^{(10)}$) and exchange (ϵ_{ex}^{HL}) terms. The values of energy components vary systematically. The absolute values for the electrostatic ($\epsilon_{el}^{(10)}$), exchange (ϵ_{ex}^{HL}), and correlation ($\epsilon_{MP}^{(2)}$) interactions increase, while the delocalization term (ΔE_{del}^{HF}) decreases as the cluster grows. The increase of the electronic density on the Li^+ cation leads to the increase of interaction energy components. The delocalization energy (ΔE_{del}^{HF}), representing interactions due to the polarization of Ar ligand in the presence of the cation electric field, is large for small clusters and decreases with an increase of cluster size as an effect of the lower charge on metal. The interactions in the largest considered complex Li^+Ar_6 are dominated by the correlation energy ($\epsilon_{MP}^{(2)}$). The comparison of total interaction energy in the complex Li^+Ar_{n-1}−Ar and dissociation energy of reaction $Li^+Ar_{n-1} + Ar = Li^+Ar_n$ indicates the importance of the geometry relaxation in the cluster formation process. The three-body interactions were studied for the complex Li^+−Ar_{n-1}−Ar. Such a selection of interacting

TABLE 4: Components of the Interaction Energy of Consecutively Attached Argon Atoms to the Remaining Part of the Complex[a]

interaction energy components	Li^+-Ar	Li^+Ar-Ar	Li^+Ar_2-Ar	Li^+Ar_3-Ar	Li^+Ar_4-Ar	Li^+Ar_5-Ar
$\epsilon_{el}^{(10)}$	0.083	0.076	−0.010	−0.193	−0.855	−1.027
ϵ_{ex}^{HL}	3.010	2.883	3.112	3.505	4.650	5.020
ΔE_{del}^{HF}	−9.017	−8.341	−7.554	−6.729	−5.368	−4.840
ΔE^{HF}	−5.924	−5.382	−4.452	−3.417	−1.572	−0.847
$\epsilon_{MP}^{(2)}$	−0.152	−0.324	−0.868	−1.540	−2.401	−3.000
ΔE^{MP2}	−6.076	−5.706	−5.320	−4.957	−3.973	−3.848

[a] All values are in kcal/mol.

TABLE 5: Three-Body Interaction Energy Components for the $Li^+-Ar_{n-1}-Ar$ Systems[a]

interaction energy components	Li^+Ar_2	Li^+Ar_3	Li^+Ar_4	Li^+Ar_5	Li^+Ar_6
$\epsilon_{el}^{(10)}$	0.168	0.252	0.516	0.594	1.045
$\epsilon_{ex,2}^{HL}$	5.807	8.876	11.278	10.671	10.869
$\epsilon_{ex,3}^{HL}$	−0.011	0.024	0.097	0.471	0.549
$\Delta E_{del,2}^{HF}$	−17.903	−26.139	−32.863	−34.221	−37.166
$\Delta E_{del,3}^{HF}$	0.590	1.349	2.013	2.241	2.499
$\epsilon_{MP,2}^{(2)}$	−0.517	−1.246	−2.180	−3.413	−4.364
$\epsilon_{MP,3}^{(2)}$	−0.007	−0.074	−0.133	−0.136	−0.152
ΔE^{MP2}	−11.873	−16.958	−21.272	−23.793	−26.720
ΔE_2^{MP2}	−12.446	−18.257	−23.249	−26.369	−29.616
ΔE_3^{MP2}	0.573	1.299	1.978	2.576	2.895

[a] All values are in kcal/mol.

fragments allows for the estimation of the importance of cooperative forces due to the attachment of the consecutive Ar atom. The three-body interactions constitute about 10% of the total interaction energy (Table 5). The main contribution to total interactions arises from the repulsive delocalization energy component ($\Delta E_{del,3}^{HF}$). Three-body exchange ($\epsilon_{ex,3}^{HL}$) and correlation ($\epsilon_{MP,3}^{(2)}$) forces are negligible.

V. Conclusions

The investigation of the Li^+Ar_n structure with the MP2-(FULL)/6-311G+(3df) method provides satisfactory results well representing available experimental data. This finding is extrapolated for larger Li^+Ar_n clusters ($n > 1$). The reported complexes are stable at the applied level of theory and deserve the future experimental efforts. The clusters of Li^+Ar_n possess the most symmetrical structures possible for particular number of Ar ligands (Figures 1 and 2). In smaller clusters ($n = 2-4$) the Ar−Ar distances are significantly longer from the bond in Ar_2 dimer indicating the little importance of the interligand interactions in the formation of structures. For Li^+Ar_5 and Li^+Ar_6 clusters the Li−Ar bond distances increase due to the shortening of ligand−ligand contacts. The bond dissociation energies for $n = 1-4$ decrease very slowly (Table 1). For this species the formation of a new Li−Ar bond does not change the bond characteristics compared to already existing bonds, and it may be considered as an additive process. The two largest clusters Li^+Ar_5 and Li^+Ar_6 are influenced by the Ar−Ar interactions due to the lack of space around the central metal cation. Their dissociation energies decrease significantly (40% on going from Li^+Ar_4 to Li^+Ar_5). The successive formation enthalpy of the Li^+Ar_6 complex increases slightly indicating the closing of the shell. The shell closing is also visible as an increase of absolute value of the incremental entropy indicating the higher rigidity of the skeleton as may be expected in the fully filled shell. The structures of Li^+Ar_n are different from H^+Ar_n complexes, which are formed as two distinguished shells (2 + 5) leading to shell closing for 7 argon atoms. The Na^+Ar_n complexes are rich in isomers which belong to different patterns of growth. The large ionic radius of Na^+ allows for formation of larger clusters, and the closing of the shell is observed in the Na^+Ar_8 moiety. The studied clusters, although representing different patterns of growth, do not excides available structural possibilities. Molecular structures of anionic clusters O^-Ar_n are additionally complicated due to the Jahn−Teller effects.[38]

The consecutive electronic density transfers from ligands to Li^+ lower systematically the charge on the lithium cation, and the systematic variation of interaction energy components is observed. The largest contribution to the interaction energy is due to the delocalization energy (ΔE_{del}^{HF}), although its importance decreases with the growth of the complex. The increasing correlation energy ($\epsilon_{MP}^{(2)}$) stabilizes larger clusters. The contribution of total three-body interactions is repulsive and is dominated by the three-body delocalization energy component ($\Delta E_{del,3}^{HF}$).

Acknowledgment. This work was supported by NSF EPSCOR Grant No. 99-01-0072-08, CREST Grant No. HRD-01-25484, Wroclaw University of Technology Grant, and the AHPCRC under the agreement number DAAH04-95-2-00003/contract number DAAH04-95-C-0008, the contents of which does not necessarily reflect the position or the policy of the government, and no official endorsement should be inferred. The Mississippi Center for Supercomputing Research and Wroclaw Supercomputing and Networking Center are acknowledged for a generous allotment of computer time.

References and Notes

(1) Wijnaendts van Resandt, R. W.; Champion, R. L. Los, J. *Chem. Phys.* **1976**, *17*, 297.
(2) Polak-Dingels, P.; Rajan, M. S.; Gislason, E. A. *J. Chem. Phys.* **1982**, *77*, 3983.
(3) Gatland, I. R. *J. Chem. Phys.* **1981**, *75*, 4162.
(4) Gatland, I. R.; Thackston, M. G.; Pope, W. M.; Eisele, F. L.; Ellis, H. W.; McDaniel, E. W. *J. Chem. Phys.* **1978**, *68*, 2775.
(5) Fiedler, J.; Frey, L.; Steigerwald, F.; Langhoff, H.; Griegel, T.; Petkau, K.; Hammer, W. *Z. Phys. D* **1989**, *11*, 141.
(6) Larsen, P.-H.; Skullerud, H. R.; Løvaas, T. H.; Stefansson, T. *J. Phys. B: At. Mol. Opt. Phys.* **1988**, *21*, 2519.
(7) Ahlrichs, R.; Böhm, H. J.; Brode, S.; Tang, K. T.; Toennies, J. P. *J. Chem. Phys.* **1988**, *88*, 6290.
(8) Iwata, S.; Nanbu, S.; Kitajima, H. *J. Chem. Phys.* **1991**, *94*, 3707.
(9) Ahmadi, G. R.; Roeggen, I. *J. Phys. B. At. Mol. Opt. Phys.* **1994**, *27*, 5603.
(10) McDowell, S. A. C. *Chem. Phys. Lett.* **1997**, *266*, 38.
(11) Kanttu, H. M.; Seetula, J. A. *Chem. Phys.* **1994**, *273*, 189.
(12) Prekas, D.; Luder, C.; Velegrakis, M. *J. Chem. Phys.* **1998**, *11*, 4450.
(13) Fridgen, T. D.; Parnis, J. M. *J. Chem. Phys.* **1998**, *109*, 2162.
(14) Giju, K. T.; Roszak, S.; Leszczynski, J. *J. Chem. Phys.* **2002**, *117*, 4803.

(15) Nagata, T.; Aoyagi, M.; Iwata, S. *J. Phys. Chem. A* **2004**, *108*, 683.

(16) Giju, K. T.; Roszak, S.; Gora, R. W.; Leszczynski, J. *Chem. Phys. Lett.* **2004**, *391*, 112.

(17) Mϕller, C.; Plesset, M. S. *Phys. Rev.* **1934**, *46*, 618.

(18) Pople, J. A.; Head-Gordon, M.; Raghavachari, K. *J. Chem. Phys.* **1987**, *87*, 5968.

(19) Bartlett, R. J.; Sekino, H.; Purvis, G. D. *Chem. Phys. Lett.* **1983**, *98*, 66.

(20) Hehre, W. J.; Radom, L.; Schleyer, P. v. R.; Pople, J. A. *Ab Initio Molecular Orbital Theory*; Wiley-Interscience: New York, 1986.

(21) Herman, P. R.; La Rocque, P. E.; Stoicheff, B. P. *J. Chem. Phys.* **1988**, *89*, 4535.

(22) Roszak, S.; Leszczynski, J. *J. Phys. Chem. A* **2003**, *107*, 949.

(23) Gutowski, M.;. van Duijneveldt, F. B.; Chalasinski, G.;. Piela, L. *Mol. Phys.* **1987**, *61*, 233.

(24) Sokalski, W. A.; Roszak, S.; Pecul, K. *Chem. Phys. Lett.* **1988**, *153*, 153.

(25) Cybulski, S. M.; Chałasiński, G.; Moszyński, R. *J. Chem. Phys.* **1990**, *92*, 4357.

(26) Jansen, H. B.; Ros, P. *Chem. Phys. Lett.* **1969**, *3*, 140.

(27) Boys, S. F.; Bernardi, F. *Mol. Phys.* **1970**, *19*, 553.

(28) Hankins, D.; Moskowitz, J. W.; Stillinger, F. H. *J. Chem. Phys.* **1970**, *53*, 4544.

(29) Kaplan, I. G. *Pol. J. Chem.* **1998**, *72*, 1454.

(30) Burcl, R.; Cybulski, S. M.; Szczesniak, M. M.; Chalasinski, G. *J. Chem. Phys.* **1995**, *103*, 299.

(31) Löwdin, P. O. *Adv. Phys.* **1956**, *5*, 1.

(32) Jeziorski, B.; Bulski, M.; Piela, L. *Int. J. Quantum Chem.* **1976**, *10*, 281.

(33) Chalasinski, G.; Szczesniak, M. M. *Chem. Rev.* **1994**, *94*, 1723.

(34) Frisch, M. J.; Trucks, G. W.; Schlegel, H. B.; Scuseria, G. E.; Robb, M. A.; Cheeseman, J. R.; Zakrzewski, V. G.; Montgomery, J. A., Jr.; Stratmann, R. E.; Burant, J. C.; Dapprich, S.; Millam, J. M.; Daniels, A. D.; Kudin, K. N.; Strain, M. C.; Farkas, O.; Tomasi, J.; Barone, V.; Cossi, M.; Cammi, R.; Mennucci, B.; Pomelli, C.; Adamo, C.; Clifford, S.; Ochterski, J.; Petersson, G. A.; Ayala, P. Y.; Cui, Q.; Morokuma, K.; Malick, D. K.; Rabuck, A. D.; Raghavachari, K.; Foresman, J. B.; Cioslowski, J.; Ortiz, J. V.; Baboul, A. G.; Stefanov, B. B.; Liu, G.; Liashenko, A.; Piskorz, P.; Komaromi, I.; Gomperts, R.; Martin, R. L.; Fox, D. J.; Keith, T.; Al-Laham, M. A.; Peng, C. Y.; Nanayakkara, A.; Challacombe, M.; Gill, P. M. W.; Johnson, B.; Chen, W.; Wong, M. W.; Andres, J. L.; Gonzalez, C.; Head-Gordon, M.; Replogle, E. S.; Pople, J. A. *Gaussian 98*, Revision A.9, Gaussian, Inc.: Pittsburgh, PA, 1998.

(35) Glendening, E. D.; Badenhoop, J. K.; Reed, A. E.; Carpenter, J. E.; Weinhold, F. *NBO 5.0*, Theoretical Chemistry Institute, University of Wisconsin, Madison, WI, 1998.

(36) Gora, R. W.; Bartkowiak, W.; Roszak, S.; Leszczynski, J. *J. Chem. Phys.* **2002**, *117*, 1031.

(37) Schmidt, M. S.; Baldridge, K. K.; Boatz, J. A.; Elbert, S. T.; Gordon, M. S.; Jensen, J. H.; Koseki, S.; Matsunaga, N.; Nguyen, K. A.; Su, S. J.; Windus, T. L.; Dupuis, M.; Montgomery, J. A. *J. Comput. Chem.* **1993**, *14*, 1347.

(38) Roszak, S.; Gora, R.; Leszczynski, J. *Chem. Phys. Lett.* **1999**, *313*, 198.